Frascati Physics Series Vol. XXXV (2004), pp. 231-239
HEAVY QUARKS AND LEPTONS - San Juan, Puerto Rico, June 1-5, 2004

MEASUREMENT OF $|V_{cb}|$ AND HQE PARAMETERS FROM SEMILEPTONIC B DECAYS

Dominique Fortin
Department of Physics and Astronomy, University of Victoria, BC, Canada.

ABSTRACT

Measurements of the CKM matrix element $|V_{cb}|$ are performed using semileptonic B decays recorded with the BaBar detector. These decays are primarily identified by the presence of a high momentum lepton. Several measurements of the hadronic mass and lepton energy moments are then performed as a function of the minimum allowed lepton energy $E_{\rm cut}$. Combining these measurements into the HQE kinetic-mass scheme allows for the simultaneous determination of the inclusive semileptonic branching ratio $\mathcal{B}(B \to X_c \ell \nu)$, $|V_{cb}|$, the b- and c-quark masses, and the HQE parameters.

1 Introduction

The element $|V_{cb}|$ of the CKM matrix is a fundamental parameter of the Standard Model and, as such, a precise measurement of $|V_{cb}|$ is important. The

weak decay rate for $B \to X_c \ell \nu$ may be calculated accurately at the parton level; it is proportional to $|V_{cb}|^2$ and also depends on the charm and bottom quark masses. In order to extract $|V_{cb}|$ from the measurements of the semileptonic B-meson decay rate, corrections to the parton-level calculations must be applied to encompass the effects of strong interactions. Heavy-Quark Expansions (HQEs) [1] have become a useful tool for calculating perturbative and non-perturbative QCD corrections [2], and for estimating their uncertainties. For instance, in the kinetic-mass scheme [3], expansions in terms of $1/m_b$ and $\alpha_s(m_b)$ to order $\mathcal{O}(1/m_b^3)$ contain six parameters: the running kinetic masses of the b- and c-quarks, $m_b(\mu)$ and $m_c(\mu)$, and four non-perturbative parameters. These parameters may be determined simultaneously from a fit to the moments of the hadronic-mass and electron-energy distributions from semileptonic B decays to charm particles. This fit yields significantly improved measurements of the inclusive branching fraction $B \to X_c \ell \nu$ and of $|V_{cb}|$ [4]. It also allows to test the consistency of the data with the HQEs employed and to check for the possible impact of higher-order contributions. In my presentation, I limited myself to the results obtained by the BaBar experiment [5], and summarize these below. New models [6, 7, 8] have recently become available and are currently under study.

2 Moments and fitting technique

The results I presented were based on moment measurements described in [9, 10] These moments were derived from the inclusive hadronic-mass (M_X) and electron energy (E_ℓ) distributions in $B \to X_c \ell \nu$ decays produced at the $\Upsilon(4S)$ resonance, and averaged over charged and neutral B. In the case of energy moments, only electrons were used, whereas muons were also used for the mass moments.

The electron-energy distribution was measured in events tagged by a high-momentum electron from the second B meson. To differentiate between primary and secondary decay electrons, the data were divided into unlike- and like-sign samples, $Q(e_{\rm tag}) = \mp Q(e_{\rm sig})$, respectively. Primary signal electrons made up most of the unlike-sign sample. Background electrons originating from the same B meson as the tagged electron usually have opposite charge and direction; they were suppressed by applying a cut on the opening angle between the two electrons. Further backgrounds from $J/\Psi \to e^+e^-$ were re-

moved by applying a veto on the invariant mass $M_{e\bar{e}}$ of the tagged electron for the interval $2.9 < M_{e\bar{e}} < 3.15$ GeV/c^2. Like-sign electrons are mostly produced in secondary decays. Energy spectra for electrons produced via photon conversion and Dalitz decays were extracted from data studies, whereas spectra for cascade $b \to c\tau\nu$ and $b \to c\bar{c}s$ electrons were estimated from Monte Carlo simulations. Continuum backgrounds, which contribute to both like- and unlike-sign samples, were subtracted out by scaling the off-resonance yields to on-resonance luminosity and energy.

The hadronic-mass distribution was measured in events tagged by the fully reconstructed hadronic decay of the second B meson, which allowed for a knowledge of the B flavour and momentum $\mathbf{p_B}$. The kinematic consistency of the $B_{\rm reco}$ candidates was checked by computing the beam-energy-substituted mass $m_{ES} = \sqrt{s/4 - \mathbf{p_B}^2}$. Combinatorial backgrounds were subtracted out from a fit to the m_{ES} distribution using an emperical function [11] describing the combinatorial background from both continuum and $B\overline{B}$ events and a narrow signal function [12] peaked at the B-meson mass. Further requirements were applied on the recoil B: the lepton charge needed to be consistent with the $B_{\rm recoil}$ flavour, and the measured missing energy and momentum had to be consistent with a neutrino. The extracted hadronic mass of the meson was then corrected for detector resolution and efficiency losses on a event-by-event basis using the linear relationships observed between the measured and generated M_X values in Monte Carlo simulations. To verify this procedure, the calibration was applied to measured masses for exclusive final states in simulated $\overline{B} \to X_c \ell \overline{\nu}$ decays and the resulting calibrated mass was compared to the true one. No significant mass bias was observed after calibration for the full mass range. The procedure was also validated on a data sample of partially reconstructed $D^{*+} \to D^0\pi^+$ decays.

All moments were measured as functions of E_{cut}, a lower limit on the lepton energy, and were corrected for detector effects and QED radiation [13]. Charmless contributions were subtracted out based on the branching fraction $B \to X_u \ell\nu$=$(0.22 \pm 0.05)\%$ [14]. The first electron energy moment, defined as $M_1^\ell(E_{cut}) = \langle E_\ell \rangle_{E_\ell > E_{cut}}$, and the second and third moments, defined as $M_n^\ell(E_{cut}) = \langle (E_\ell - M_1^\ell(E_{cut}))^n \rangle_{E_\ell > E_{cut}}$ with n =2,3, were measured. In addition, the partial branching fraction $M_0^\ell(E_{cut}) = \int_{E_{cut}}^{E_{max}} (d\mathcal{B}_{c\ell\nu}/dE_\ell)\, dE_\ell$ was also obtained. The hadronic-mass moments $M_n^X(E_{cut}) = \langle m_X^n \rangle_{E_\ell > E_{cut}}$ were

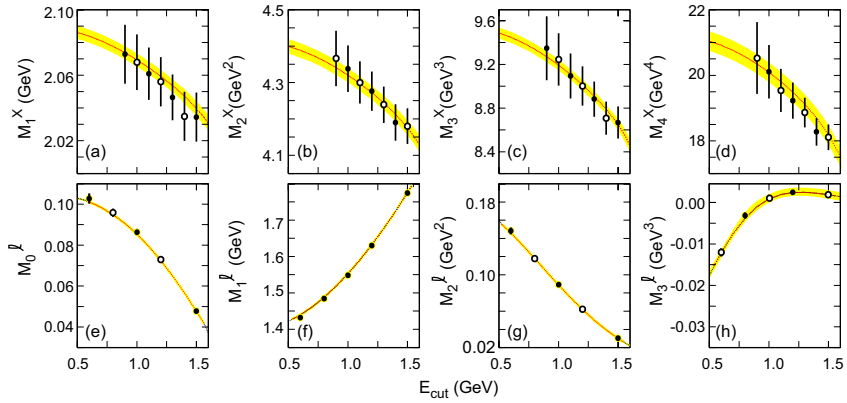

Figure 1: *The measured hadronic-mass (a-d) and electron-energy (e-h) moments as a function of the cut-off energy, E_{cut}, compared with the result of the simultaneous fit (line), with the theoretical uncertainties* [16] *indicated as shaded bands. The solid data points mark the measurements included in the fit. The vertical bars indicate the experimental errors. Moment measurements for different E_{cut} are highly correlated.*

measured for n =1,2,3,4. The measured electron-energy and hadronic-mass moments as a function of E_{cut} are shown in Fig. 1.

In the kinetic-mass scheme the HQE to $\mathcal{O}(1/m_b^3)$ for the rate of $B \to X_c \ell\nu$ decays can be expressed as [15]

$$\Gamma_{c\ell\nu} = \frac{G_F^2 m_b^5}{192\pi^3}|V_{cb}|^2(1+A_{ew})A_{pert}(r,\mu)\times \left[z_0(r)\left(1-\frac{\mu_\pi^2-\mu_G^2+\frac{\rho_D^3+\rho_{LS}^3}{m_b}}{2m_b^2}\right) -2(1-r)^4\frac{\mu_G^2+\frac{\rho_D^3+\rho_{LS}^3}{m_b}}{m_b^2}+d(r)\frac{\rho_D^3}{m_b^3}+\mathcal{O}(1/m_b^4)\right]. \quad (1)$$

The leading non-perturbative effects arise at $\mathcal{O}(1/m_b^2)$ and are parameterized by $\mu_\pi^2(\mu)$ and $\mu_G^2(\mu)$, the expectation values of the kinetic and chromomagnetic dimension-five operators. At $\mathcal{O}(1/m_b^3)$, two additional parameters enter, $\rho_D^3(\mu)$ and $\rho_{LS}^3(\mu)$, the expectation values of the Darwin (D) and spin-orbit

(LS) dimension-six operators. These parameters depend on the scale μ[1] that separates short-distance from long-distance QCD effects. Electroweak corrections are $1 + A_{ew} \approx 1.014$, and perturbative QCD corrections are estimated to be $A_{pert}(r, \mu) \cong 0.91 \pm 0.01$ [15]. Linearized expressions for the HQEs [16] were then substitued into equation 1.

HQEs in terms of the same heavy-quark parameters are available for the hadronic-mass and electron-energy moments. The dependence on the heavy-quark parameters was again linearized using the same *a priori* estimates of the parameters [15, 16]. The differences between the linearized expressions and the full theoretical calculation were shown to be small in all cases. These linear equations allowed for the determination of the unknown heavy-quark parameters, the total branching fraction $\mathcal{B}(B \to X_c \ell \nu)$, and $|V_{cb}|$ from a simultaneous χ^2 fit to the measured moments and the partial branching fraction, all as a function of the cut-off lepton energy, E_{cut}.

In total, four hadronic-mass moments for each of seven different values of E_{cut}, ranging from 0.9 to 1.5 GeV, and three electron-energy moments plus the partial branching fraction at five values of E_{cut}, ranging from 0.6 to 1.5 GeV, were available [9, 10]. Many of these individual moments were highly correlated such that a set of moments for which the correlation coefficients do not exceed 95% was chosen. As a result, only half of the 28 mass moments and 13 of the 20 energy moments were kept for the fit.

3 Results

The global fit took into account the statistical and systematic errors and correlations of the individual measurements, as well as the uncertainties of the expressions for the individual moments. As suggested in [16], the uncertainty of the calculated moments was assesed by varying in the linearized expressions the *a priori* estimates for μ_π^2 and μ_G^2 by $\pm 20\%$ and for ρ_{LS}^3 and ρ_D^3 by $\pm 30\%$. For a given moment, these changes were assumed to be fully correlated for all values of E_{cut}, but uncorrelated for different moments. The resulting fit, shown in fig. 1, describes the data well with $\chi^2 = 15.0$ for 20 degrees of freedom. Table 1 lists the fitted parameters and their errors. Note that for the mass difference, BaBar obtained $m_b - m_c = (3.436 \pm 0.025_{exp} \pm 0.018_{HQE} \pm 0.010_{\alpha_s})$ GeV.

[1] Calculations are performed for $\mu = 1$ GeV [3].

Table 1: *Fit results and error contributions from the moment measurements, approximations to the HQEs, and additional theoretical uncertainties from α_s terms and other perturbative and non-perturbative terms contributing to $\Gamma_{c\ell\nu}$.*

Parameter	Result	δ_{exp}	δ_{HQE}	δ_{α_s}	δ_Γ
$\|V_{cb}\|$ (10^{-3})	41.390	0.437	0.398	0.150	0.620
m_b (GeV)	4.611	0.052	0.041	0.015	
m_c(GeV)	1.175	0.072	0.056	0.015	
μ_π^2 (GeV^2)	0.447	0.035	0.038	0.010	
ρ_D^3 (GeV^3)	0.195	0.023	0.018	0.004	
μ_G^2 (GeV^2)	0.267	0.055	0.033	0.018	
ρ_{LS}^3 (GeV^3)	-0.085	0.038	0.072	0.010	
$\mathcal{B}(B \to X_c\ell\nu)$ (%)	10.611	0.163	0.063	0.000	

Beyond the uncertainties that are included in the fit, the limited knowledge of the expression for the decay rate, including various perturbative corrections and higher-order non-perturbative corrections, introduces an error in $|V_{cb}|$, assessed to be 1.5% [15]. On the other hand, the uncertainty in α_s is estimated to have a relatively small effect.

The fit results are fully compatible with independent estimates [16] of μ_G^2=(0.35±0.07) GeV^2, based on the B^*-B mass splitting, and of ρ_{LS}^3=(−0.15± 0.10) GeV^3, from heavy-quark sum rules [17]. Figure 2 shows the $\Delta\chi^2 = 1$ ellipses for $|V_{cb}|$ versus m_b and μ_π^2, for a fit to all moments and separate fits to the electron-energy moments and the hadronic-mass moments, but including the partial branching fractions in both. The lepton-energy and hadronic-mass moments have slightly different sensitivity to the fit parameters, but the results for the separate fits are fully compatible with each other and with the global fit to all moments. Since the expansions for the two sets of moments are sensitive to different theoretical uncertainties and assumptions, in particular the differences in the treatment of the perturbative corrections, the observed consistency of the separate fits indicates that such differences are small compared with the experimental and assumed theoretical uncertainties.

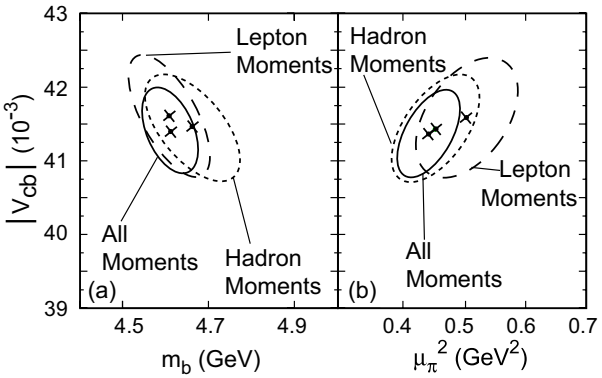

Figure 2: *Fit results (crosses) with contours corresponding to* $\Delta\chi^2 = 1$ *for two pairs of the eight free parameters a)* m_b *and b)* μ_π^2 *versus* $|V_{cb}|$*, separately for fits using the hadronic-mass, the electron-energy, and all moments.*

4 Conclusion

BaBar extracted $|V_{cb}|$, the semileptonic branching fraction, and the heavy-quark masses,

$$\begin{aligned} |V_{cb}| &= (41.4 \pm 0.4_{exp} \pm 0.4_{HQE} \pm 0.6_{th}) \times 10^{-3}, \\ \mathcal{B}_{ce\nu} &= (10.61 \pm 0.16_{exp} \pm 0.06_{HQE})\%, \\ m_b(1\text{ GeV}) &= (4.61 \pm 0.05_{exp} \pm 0.04_{HQE} \pm 0.02_{th})\text{ GeV}, \\ m_c(1\text{ GeV}) &= (1.18 \pm 0.07_{exp} \pm 0.06_{HQE} \pm 0.02_{th})\text{ GeV}, \end{aligned}$$

as well as the non-perturbative parameters in the kinetic-mass scheme up to order $(1/m_b^3)$.

Based on a large set of hadronic-mass and electron-energy moments and a consistent set of HQE calculations, uncertainties in the $\mathcal{O}(1/m_b^3)$ terms were determined from the data without constraints to any *a priori* values. The fitted values of the parameters appear to be consistent with theoretical estimates [3, 15], and the uncertainties on the quark masses are much smaller than those of previous measurements [18]. Finally, the result on $|V_{cb}|$ is in agreement with previous measurements using HQEs, either for a different mass scheme and with fixed terms of $\mathcal{O}(1/m_b^3)$ [7], or for the kinetic-mass scheme,

but with external constraints on almost all HQE parameters [8], as well as with an analysis combining both of these measurements [6].

References

1. M. Voloshin and M. Shifman, Sov. J. Nucl. Phys. **41**, 120 (1985); J. Chay, H. Georgi, and B. Grinstein, Phys. Lett. **B247**, 399 (1990); I. I. Bigi, and N. Uraltsev, Phys. Lett. **B280**, 271 (1992).
2. I. I. Bigi, N. Uraltsev, and A. I. Vainshtein, Phys. Lett. **B293**, 430 (1992); I. I. Bigi, M. Shifman, N. Uraltsev, and A. Vainshtein, Phys. Rev. Lett. **71**, 496 (1993); B. Blok, L. Koyrakh, M. Shifman, and A. Vainshtein, Phys. Rev. **D49**, 3356 (1994); A. V. Manohar and M. B. Wise, Phys. Rev. **D49**, 1310 (1994); M. Gremm and A. Kapustin, Phys. Rev. **D55**, 6924 (1997).
3. I. I. Bigi, M. Shifman, N. Uraltsev, and A. Vainshtein, Phys. Rev. **D56**, 4017 (1997).
4. B. Aubert *et al.* [BaBar Collaboration], Phys. Rev. **D67**, 031101 (2003).
5. B. Aubert *et al.* [BaBar Collaboration], Phys. Rev. Lett. **93**, 011803 (2004).
6. C. W. Bauer, Z. Ligeti, M. Luke and A. V. Manohar Phys. Rev. **D67**, 054012 (2003).
7. A. H. Mahmood *et al.* [CLEO Collaboration], Phys. Rev. **D67**, 072001 (2003) .
8. M. Battaglia *et al.* [DELPHI Collaboration], Phys. Lett. **B556**, 41 (2003).
9. B. Aubert *et al.* [BaBar Collaboration], Phys. Rev. D **69**, 111104 (2004).
10. B. Aubert *et al.* [BaBar Collaboration], Phys. Rev. D **69**, 111103 (2004).
11. H. Albrecht *et al.* [ARGUS Collaboration], Phys. Lett. **B185**, 218 (1987).
12. T.Skwatnicki *et al.* [Crystal Ball Collaboration], DESY F31-86-02 (1986).
13. E. Barbiero and Z. Was, Comput. Phys. Comm. **79**, 291 (1994).
14. B. Aubert *et al.* [BaBar Collaboration], Phys. Rev. Lett. **92**, 071802 (2004).

15. D. Benson, I. I. Bigi, T. Mannel, and N. Uraltsev, Nucl. Phys. **B665**, 367 (2003).

16. P. Gambino and N. Uraltsev, *Moments of Semileptonic B Decay Distributions in the* $1/m_b$ *Expansion*, hep-ph/0401063, to be published in Eur. Phys. J. C (2004).

17. I. I. Bigi, M. A. Shifman, and N. G. Uraltsev, Ann. Rev. Nucl. Part. Sci., **47**, 591 (1997).

18. K. Hagiwara *et al.* Phys. Rev. **D66**, 010001 (2002).